



---

## PROCESS FOR DETECTION OF METAL-CONTAINING NANOPARTICLES IN WASTEWATER TREATMENT

G. ALEKHYA, CH. ASHOK, K. VENKATESWARA RAO,  
CH. SHILPA CHAKRA

Centre for Nano Science and Technology, Institute of Science and  
Technology, Jawaharlal Nehru Technological University Hyderabad,  
Kukatpally, Hyderabad-500085, Telangana, India.

Corresponding E-mail: [golla.alekhya92@gmail.com](mailto:golla.alekhya92@gmail.com)

### ABSTRACT

The unique properties of engineered nanomaterial's (ENM's) make them attractive for plethora of applications. Since the ENM's are incorporated into a growing variety of products ranging from common household items to novel medical technologies, their potential to enter the environment and biological systems is increasing. This invokes concerns for the equally unique human and environmental risks associated with the use of these materials, hence nanoparticles (NP's) determination and treatment (or removal) techniques in environment (air, water, soil) has recently gained considerable interest. This paper reviews on the product-centric models for the flow of ENM's and based on the predicted environmental concentration (PEC) modelling, the major routes for the environmental exposure of the ENM's were found as Wastewater treatment plant (WTP) effluents/sludge. The wastewater after undergoing secondary treatment still contains NP's. Here some detection techniques of metal-containing nanoparticles (NPs) including field-flow fraction (FFF), Hydro Dynamic Chromatography (HDC) and quantification techniques like inductively coupled plasma-mass spectrometry (ICP-MS) are reviewed.

**Keywords:** Metal-containing Nanoparticles, WTP, ENM's, PEC, FFF, HDC.

### Introduction:

Nanotechnology often deals with materials having at least one of its dimensions in nanoscale i.e., 1 to 100 nm. These materials with increased surface to volume ratio are known nanomaterials. Engineered nanomaterials (ENM's) are intentionally produced with specific properties. Due to the increased surface area of ENM's their properties like reactivity, electrical conductivity, mechanical strength, magnetic properties and optical properties are varied greatly compared to the bulk properties. Hence ENM'S find many



applications and so the production and use of ENM's is rapidly increasing. The Project on Emerging Nanotechnologies, which keeps track of consumer products containing nanotechnology, lists a total of 1,628 products and applications which have been introduced to the market since 2005, this represents an increase of 24% since 2010 as shown in figure 1.

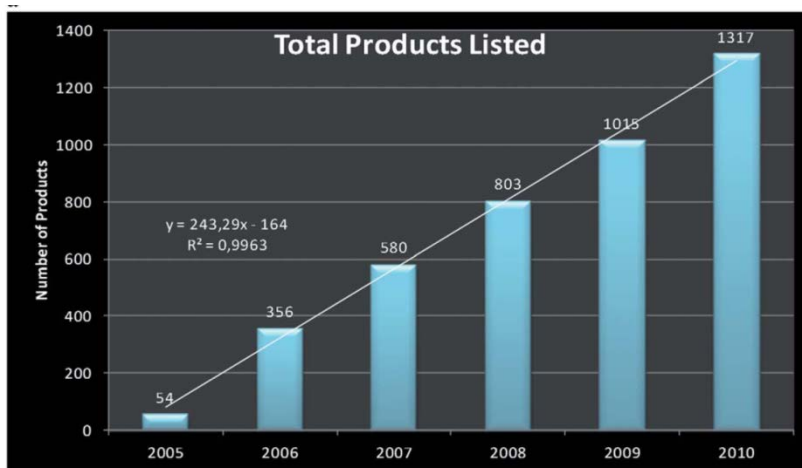


Figure 1 Estimated number of total products listed since 2005 to 2010 that contain ENMs in varying amounts.  
(<http://www.nanotechproject.org/inventories/consumer>)

Now observing the lifecycle of the ENM's including manufacturing, exposure/usage of products and their postuse release and migration in the environment. We come to know that at each stage in their lifecycle, there is a risk of entering nanomaterials into the environment as shown in fig 2 (a). Into what environmental compartments majorly the ENMs flow is given by material flow modelling general framework as shown in figure 2 (b). The risks due to ENM emissions can be estimated if both exposure and hazard are observed. Some studies estimate the risk by a parameter known as risk quotient, which is the ratio of PEC value to predicted no-effect environmental concentration (PNEC) value. A risk quotient greater than or equal to 1 indicates the potential for risk and requires further testing, whereas quotients less than 1 imply that risks are currently not to be expected. Risk quotients of approximately 1 or higher in surface water were computed for nano-TiO<sub>2</sub>. Quotients of approximately 1 for nano-Ag and significantly greater than 1 were modelled for nano-TiO<sub>2</sub>, nano-ZnO, and nano-Ag in undiluted effluents of sewage treatment plants (Nicole C. Mueller and Bernd Nowack, 2008).

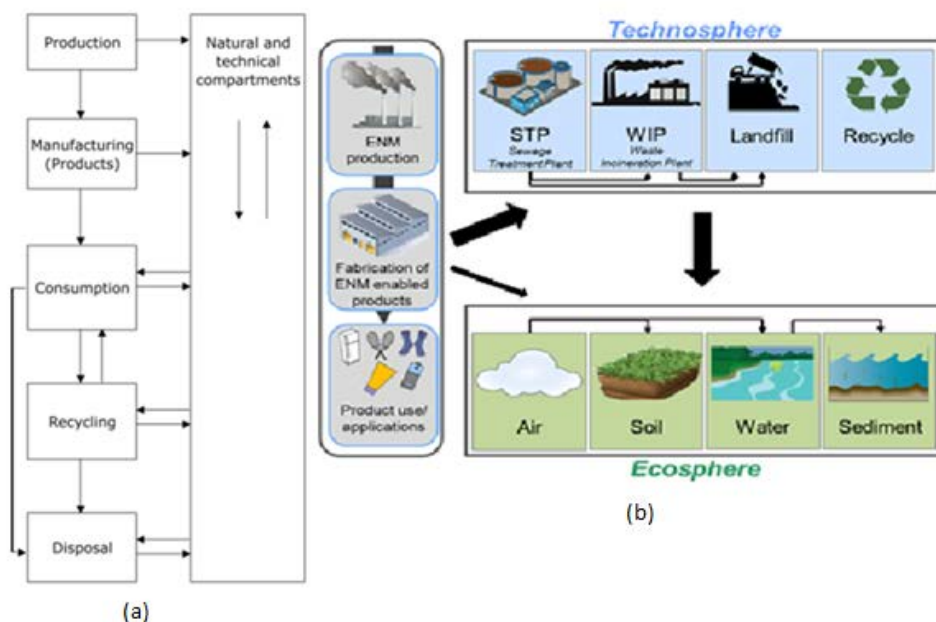


Figure 2(a) Schematic showing the flow of NPs at each stage of their life cycle into environmental compartments, 2(b) General concept of material flow modelling with detailed view of environmental compartments and flow of NPs among themselves.

How these ENM's flow into environmental compartments(material-flow modelling) like sewage treatment plant (STP)/wastewater treatment plant (WTP)/waste incineration plant (WIP)/landfills and at what concentrations they exist in environmental matrices-predicted environmental concentrations (PEC), and material specific concentration limits-PEC & Probabilistic species sensitivity distributions (PSSD). All these aspects were studied through a series of frameworks and case studies, (Fadri Gottschalk, 2013 et al., Troy M. Benn and Paul Westerhoff, 2008 et al., Gottschalk F, 2011 et al., Christine Ogilvie Hendren, 2013 et al., S. Gavankar, 2014 et al.) especially on the flows of the five most used ENM's (nano-TiO<sub>2</sub>, nano-ZnO, nano-Ag, CNT and fullerenes) in U.S, EU, and Switzerland regions and finally listed the PEC values for all the five ENM's as shown below in figure 3. From which we conclude that nano-TiO<sub>2</sub> and nano-ZnO are mostly found in STP effluent (Tian yin sun, 2014 et al.). Now if we focus on analytical techniques to estimate their concentration values. Till now no standard analytical techniques to detect and quantify the amount or concentrations of ENM's in complex environmental matrices like STP effluent and wastewater, landfills etc., are present. However number of



studies was carried out on the detection/separation techniques like FFF, cross-flow-fractionation (CFF), chromatography, ultrafiltration, ultracentrifugation, capillary exclusions and many others. Out of these many papers are available on FFF, asymmetrical flow FFF (AF4) and HDC techniques (Ana Lopez-Serrano, 2013 et al.).

Figure 3 Predicted ENM concentrations in different technical and environmental compartments shown as mode (most frequent value) and as a range of lower and upper percentiles ( $Q_{0.15}$  and  $Q_{0.85}$ ). Black values designate concentrations; grey values designate yearly increases in concentrations. ENM concentrations in surface water and sediments represent no and complete sedimentation, respectively.

(Environmental Pollution 185 (2014) 69-76)

	EU			Switzerland				EU			Switzerland				
	Mode	$Q_{0.15}$	$Q_{0.85}$	Mode	$Q_{0.15}$	$Q_{0.85}$		Mode	$Q_{0.15}$	$Q_{0.85}$	Mode	$Q_{0.15}$	$Q_{0.85}$		
<b>Nano-TiO<sub>2</sub></b>															
STP Effluent	16	13	110	32	26	220	µg/L	STP Effluent	4.0	3.6	12	5.5	4.9	16	ng/L
Surface water	0.53	0.40	1.4	0.67	0.54	3.0	µg/L	Surface water	0.23	0.17	0.35	0.35	0.27	0.56	ng/L
Sediment	1.9	1.4	4.8	2.3	1.9	10	mg/kg y	Sediment	0.79	0.61	1.2	1.2	0.95	2.0	µg/kg y
STP sludge	170	150	540	320	250	950	mg/kg	STP sludge	0.15	0.12	0.23	0.27	0.21	0.40	mg/kg
Natural and urban soil	0.13	0.09	0.24	0.57	0.39	1.0	µg/kg y	Natural and urban soil	5.1	3.7	7.1	22	17	32	ng/kg y
Sludge treated soil	1200	940	3600				µg/kg y	Sludge treated soil	0.99	0.76	1.6				µg/kg y
Air	0.001	0.000	0.001	0.002	0.002	0.004	µg/m <sup>3</sup>	Air	0.02	0.02	0.03	0.09	0.07	0.13	ng/m <sup>3</sup>
Solid waste	12	8.3	20	19	14	32	mg/kg	Solid waste	1.7	1.3	2.6	3.0	2.3	4.0	mg/kg
WIP bottom ash	120	82	230	210	150	410	mg/kg	WIP bottom ash	0.23	0.21	1.4	0.39	0.36	2.3	mg/kg
WIP fly ash	150	110	310	280	200	560	mg/kg	WIP fly ash	0.36	0.33	2.9	0.60	0.55	4.7	mg/kg
<b>Nano-ZnO</b>															
STP Effluent	2.3	1.7	21	5.3	3.7	45	µg/L	STP Effluent	1.7	1.3	7	3.4	2.3	13	ng/L
Surface water	0.09	0.05	0.29	0.12	0.07	0.61	µg/L	Surface water	0.11	0.07	0.28	0.13	0.08	0.33	ng/L
Sediment	0.32	0.18	1.0	0.41	0.26	2.1	mg/kg y	Sediment	0.37	0.24	0.99	0.45	0.27	1.2	µg/kg y
STP sludge	24	17	110	45	31	200	mg/kg	STP sludge	0.09	0.05	0.22	0.15	0.09	0.34	mg/kg
Natural and urban soil	0.01	0.01	0.03	0.05	0.03	0.13	µg/kg y	Natural and urban soil	0.10	0.07	0.23	0.18	0.10	0.33	ng/kg y
Sludge treated soil	0.01	0.01	0.03				µg/kg y	Sludge treated soil	0.62	0.38	1.5				µg/kg y
Air	<0.001	<0.001	<0.001	<0.001	<0.001	<0.001	µg/m <sup>3</sup>	Air	0.001	0.000	0.001	0.001	0.000	0.001	ng/m <sup>3</sup>
Solid waste	0.89	0.47	2.4	1.6	0.73	3.7	mg/kg	Solid waste	0.07	0.04	0.13	0.08	0.04	0.14	mg/kg
WIP bottom ash	3.5	1.9	11	5.1	2.9	16	mg/kg	WIP bottom ash	0.01	0.01	0.07	0.01	0.01	0.08	mg/kg
WIP fly ash	2.8	2.7	22	4.8	4.1	33	mg/kg	WIP fly ash	0.01	0.01	0.14	0.01	0.01	0.16	mg/kg
<b>Nano-Ag</b>															
STP Effluent	0.17	0.06	16	0.32	0.08	23	ng/L	STP Effluent	0.17	0.13	7	3.4	2.3	13	ng/L
Surface water	0.66	0.51	0.94	0.45	0.37	0.73	ng/L	Surface water	0.11	0.07	0.28	0.13	0.08	0.33	ng/L
Sediment	2.3	1.8	3.3	1.6	1.3	2.6	µg/kg y	Sediment	0.37	0.24	0.99	0.45	0.27	1.2	µg/kg y
STP sludge	0.02	0.01	0.08	0.04	0.02	0.16	mg/kg	STP sludge	0.09	0.05	0.22	0.15	0.09	0.34	mg/kg
Natural and urban soil	1.2	0.91	1.8	5.1	3.9	7.4	ng/kg y	Natural and urban soil	0.10	0.07	0.23	0.18	0.10	0.33	ng/kg y
Sludge treated soil	0.11	0.09	0.65				µg/kg y	Sludge treated soil	0.62	0.38	1.5				µg/kg y
Air	0.003	0.003	0.004	0.01	0.01	0.02	ng/m <sup>3</sup>	Air	0.001	0.000	0.001	0.001	0.000	0.001	ng/m <sup>3</sup>
Solid waste	0.06	0.05	0.08	0.05	0.04	0.07	mg/kg	Solid waste	0.07	0.04	0.13	0.08	0.04	0.14	mg/kg
WIP bottom ash	0.23	0.18	0.36	0.21	0.17	0.33	mg/kg	WIP bottom ash	0.01	0.01	0.07	0.01	0.01	0.08	mg/kg
WIP fly ash	0.38	0.24	0.85	0.33	0.22	0.77	mg/kg	WIP fly ash	0.01	0.01	0.14	0.01	0.01	0.16	mg/kg

Coming to quantification techniques inductively coupled plasma-mass spectroscopy (ICP-MS) was mostly discussed and reliable technique. Especially single particle ICP-MS results were found to be matched with PEC values. Based on these detection and quantification techniques,



hyphenated techniques are evolved for estimating concentration values of metal-containing nanoparticles in STP effluents.

### ***Analytical techniques for nanomaterials characterization:***

Fundamentally there are 9 key parameters for nanomaterial's that characterize their uniqueness. They are: size, shape, concentration, structure, composition, surface functionality (porosity, surface area), surface specification (surface charge), agglomeration and size distribution. Instability of nanoparticles is well known. They can be very reactive depending on the composition of the surrounding media. Furthermore, these properties can change during sample manipulation, storage, residence within the biological system. These changes may greatly influence nanoparticle uptake and/or behaviour. Several techniques are used for a suitable extraction, separation and fractionation of nanoparticles during pre-quantification like cloud point extraction (CPE), CFF, FFF, ultrafiltration, ultracentrifugation and chromatographic techniques. Some of the most employed techniques are briefly explained below:

### **Field-flow fractionation:**

Field flow fractionation (FFF) is a family of high-resolution elution techniques which can size separate nanoparticles in the 1-100 nm range and colloids of submicron range. By use of either FFF theory or calibration with size standards, the technique can be utilized to determine particle size (Marcus. N Myers, 1997 et al.). The separation process is similar to chromatography except that the separation is based on the external field applied as opposed to chemical interactions. Depending on the type of analysis that is being performed, a different member of the FFF family can be chosen to achieve optimal separation results. The three FFF techniques that are commercially available, and thus most commonly used, include thermal FFF (ThFFF), sedimentation FFF (SdFFF), and flow FFF (FIFFF) (Korin D. Caldwell, 2000 et al.). Flow FFF can be used in either the symmetrical (FIFFF) or asymmetrical (AF4) modes and is the most widely used subset of techniques for environmental applications. It is highly versatile for a range of both natural and manufactured NPs.

The theory of separation is explained as follows: FFF is characterized by the use of an external field applied perpendicularly to the direction of sample flow through an empty, thin ribbon like channel. Due to the high aspect ratio of the FFF channel a laminar parabolic flow profile develops,

flows velocity increasing from near zero at the channel walls to a maximum at the centre of the channel as shown in figure 4. The external field drives the sample towards the bottom (accumulation) wall which tends to increase in the concentrations at the bottom wall. A counteracting diffusive force develops and drives the sample back towards the centre of the channel. Retention occurs when the analytes reside in the flow velocity zones slower than the average flow velocity of the carrier liquid passing through the channel. Hence separation occurs because different analytes reside in different flow velocity zones.

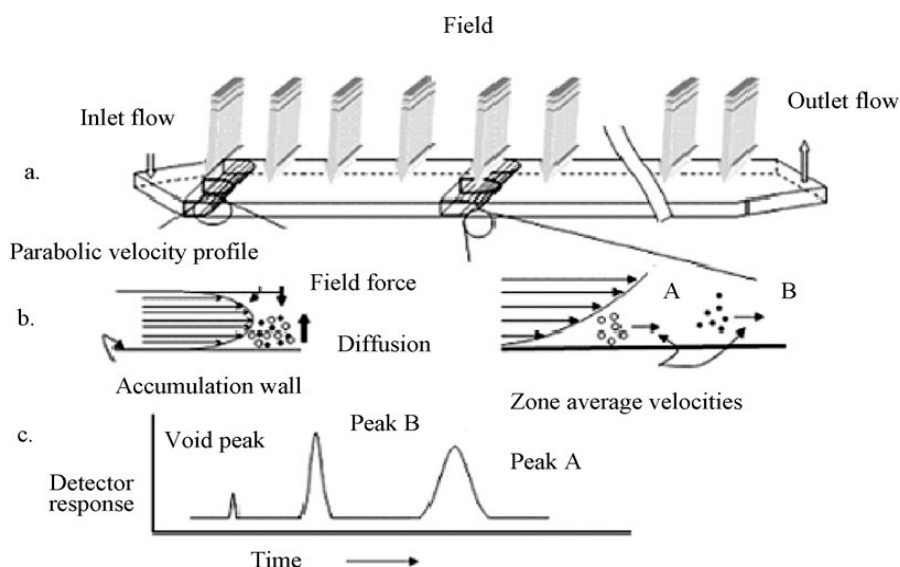


Figure 4(a) Schematic representation of an FFF channel cut-out, 4(b) exploded views of the normal mode separation mechanism of two components A and B (faster diffusing B components are located at higher elevation in faster flow velocity streamlines and are thus eluted earlier than slower diffusing A components) and 4(c) a typical FFF fractogram. (ProgPolymSci, 2009)

Three different modes of operation can occur in FFF namely normal mode, steric mode, hyper layer mode (Schimpf ME, 2000 et al., Jana Plockova, 1999 et al.) as shown in fig 4.

**Normal mode:** This is most widely used mechanism to separate analytes of size smaller than  $1\mu\text{m}$ . In this mode smaller components elute earlier than larger components.

**Steric mode:** Is applicable for components larger than  $1\mu\text{m}$  where diffusion becomes negligible and retention is governed by the distance of closest approach to the accumulation wall. Here the elution order is from largest to smallest.

**Lift or Hyper layer mode:** mode is one in which lift forces drive sample components to higher velocity streams located more than one particle radius from the accumulation wall. These hydrodynamic lift forces occur when high flow velocities are used. The elution order is the same as in the steric mode.

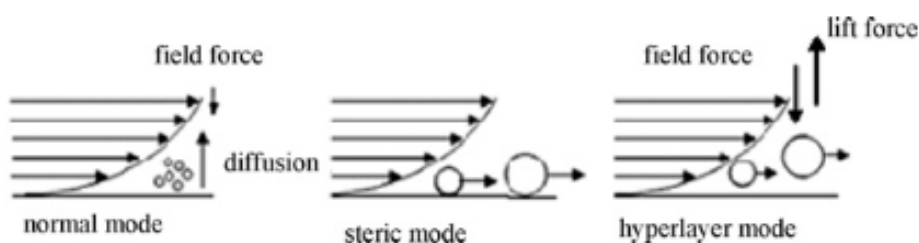


Figure 5: Schematic representation of different modes of operation that can occur in FFF. (ProgPolymSci, 2009)

#### **FIFFF:**

FIFFF was introduced in 1976 by Giddings. In this first form of flow FFF, the channel spacer is clamped between two parallel plastic blocks fitted with porous ceramic frits in each wall. A cross-flow is applied as the 'field' perpendicular to the channel flow. Cross-flow enters the channel through the porous frit on the top wall and exits the channel through an ultrafiltration membrane, overlaying a second porous frit at the bottom wall (the accumulation wall). When selecting a membrane, membrane thickness, smoothness, chemical and mechanical stability, as well as the solute size/molecular weight and interactions between solute and membrane, should be carefully considered.

#### **AF4:**

The asymmetrical version, AF4, was first introduced in 1987. A membrane is also used here as the accumulation wall. However, AF4 differs from FIFFF in that the channel has only a single permeable wall (the accumulation wall). The upper porous wall is replaced by a solid wall that is impermeable to the carrier liquid. A single channel inlet flow is split into the channel flow and the cross-flow. The ratio between the two depends on operator controlled in-line flow resistances. A schematic representation



comparing FIFFF and AF4 is shown in figure. AF4 has the following advantages over FIFFF: simpler construction and the ability to visualize the sample through a transparent upper wall (Karl Gustav Wahlund, 1987 et al.).

Because of its extraordinary resolution and applicability to a wide range of sizes, FFF has been used to separate various ENMs. As FFF offers the separation of particles with different sizes and reduced sample complexity, different-sized particles can be analyzed individually after separating the samples with FFF. Besides, unlike the chromatographic methods, the absence of a stationary phase avoids irreversible interaction with the analytes, so the morphology and the size of the NPs are preserved during operations. The fractionation of the samples can be further determined by many detectors, and on-line detectors include ultraviolet-visible spectroscopy (UV-Vis), fluorescence, light scattering, ICP-MS, while offline detectors include transmission electron microscopy (TEM), scanning electron microscopy (SEM), atomic force microscopy (AFM), atomic absorption spectrophotometry (AAS) and light scattering.

Lead, et al. utilized flow FFF to test the particle-size distributions of AgNPs at environmentally relevant levels. Thermal FFF used to separate several NPs, including Ag, Au, Pd, and Pt, and also evaluated the factors that influenced retention behaviour (M. Baalousha, 2008 et al.). The separation of AgNPs by using sedimentation FFF. However FFF techniques require often long method developments (laborious) and long durations. To acquire perfect conditions and good separation efficiency for the particles tested, a series of parameters have to be optimized, including carrier liquids, membranes, channel dimensions, and external field (Sun Tae Kim, 2007 et al.).

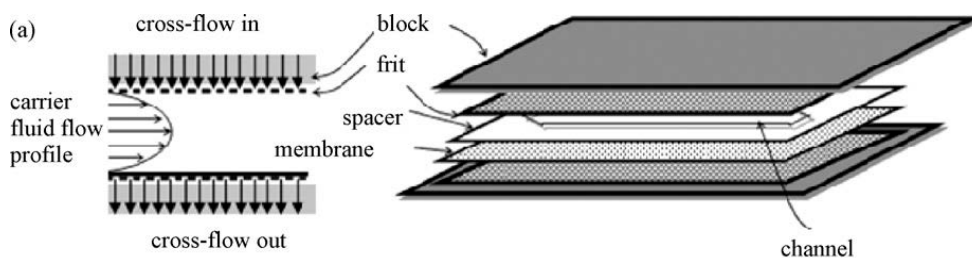
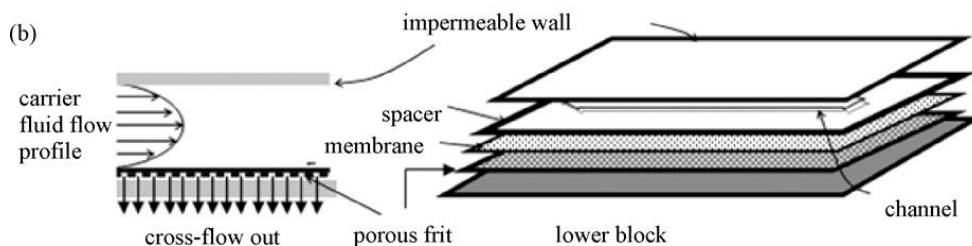


Figure 6(a) A schematic representation of Symmetric (FIFFF)



6(b) Asymmetric (AsFIFFF) channel structures  
(ProgPolymSci, 2009)

### HDC:

HDC is the technique adopted for separation of two immiscible compounds forming colloids or it can be defined as the method that separates and sizes solutes or particulates in the submicron range (30 nm-60 $\mu$ m) at high dilution, without being affected by their density (DosRamos JG, 1990 et al.). This technique includes mobile phase (gas/liquid) and stationary phase (solid/liquid) in an open narrow/widely spread column packed with non-porous microparticles to limit the interactions of nanoparticles with the bed. The separation is achieved by flow velocity and the velocity gradient across them (Striegel AM, 2012 et al.). Larger components are eluted earlier to smaller ones. The first fundamental work was published by small in 1974. In HDC the key value is separation factor  $R_F$  for a given particle of diameter  $D_p$ .  $R_F$  is the ratio of the highest elution volume ( $V_m$ ) to that measured for this particle ( $V_p$ ). A calibration curve is obtained by plotting the graph of  $D_p$  versus  $R_F$ . An important parameter to design HDC columns is a retention factor. Retention factor or capacitance factor is the ratio of time spent by the solute in the stationary phase to time spent in mobile phase. Elution of sample depends on size and porosity of packing beads, eluent flow rate, ionic strength,  $P^H$  and additives such as surfactants (Penlidis A, 1983 et al.).

The detectors used with HDC are traditionally differential refractometers or UV detectors. Other detection methods include particle-counting detection using laser scattering, multi-angle light scattering, DLS and viscosimetry. Unfortunately, the detection limit of these detectors is well above ng L<sup>-1</sup>.

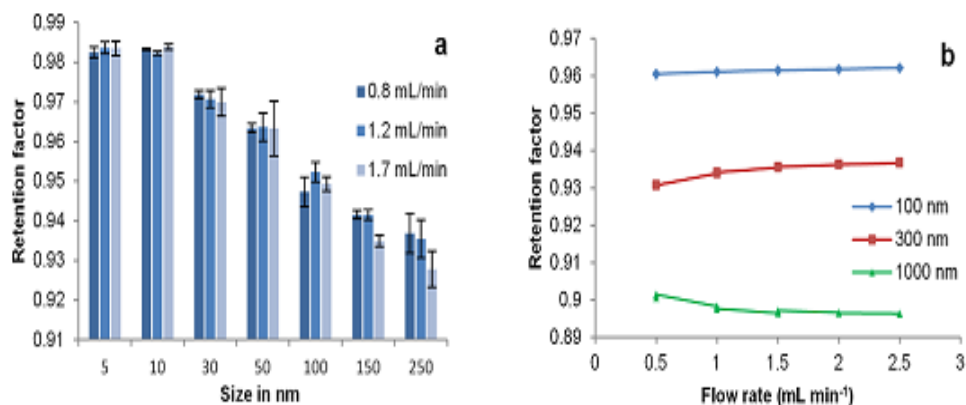


Figure 7(a) Retention factors of gold nanoparticle standards measured using HDC at different flow rates (column type 1; 3 replicates for 1.7 mL min<sup>-1</sup> and 2 replicates for the other flow rates band), 7(b) Retention factors of polystyrene standards (nominal diameters: 100 nm, 300 nm and 1000 nm) measured at different flow rates (column type 2, two replicates per suspension and flow rate value).

doi:10.1371/journal.pone.0090559.g001

The main advantages of HDC are: rapid (10 min) and convenient method, direct analysis of the original colloid medium and the use of high dilutions avoid modification of a sample which may be observed in a dry state and any effect of interactions. Existence of a unique, universal calibration curve allows calculation of  $D_p$  and PSD for any sample.

However, there are some difficulties related to the proper choice of operating variables. It is obvious that length and diameter of column play a role on resolution and domain of measurement. Particle size may affect the total recovery of material (with packed columns). Moreover, it may act on the detector response. In consequence, the PSD might be affected by the incomplete recovery of particles, due to adsorption effects, mainly for larger particles. The interpretation of data assumes that particles are spherical, although equivalence has been found for elongated structures (1  $\mu\text{m}$  particles appear as spheres of 153 nm diameters). Finally, soft materials may be deformed under the high rate of shear in packed column and orientation in flow may affect the apparent size.

## ICP-MS:

ICP-MS is a highly sensitive analytical technique widely used for ultratrace metal determination in a wide range of samples. An ICP-MS combines a high temperature ICP source converts the atoms of the elements in the sample to ions. These ions are then detected by the mass spectrometer. Once the sample aerosol is introduced into the ICP torch, it is completely desolvated and the elements in the aerosol are converted first into gaseous atoms and then ionized towards the end of the plasma. Once the elements in the sample are converted into ions, they are then brought into the mass spectrometer via the interface cones. Once the ions enter the mass spectrometer, they are separated by their mass-to-charge ratio. The most commonly used type of mass spectrometer is the *quadrupole massfilter*. ICP-MS is often considered to have simultaneous multi elemental analysis properties. The schematic of ICP-MS is as shown below in figure.

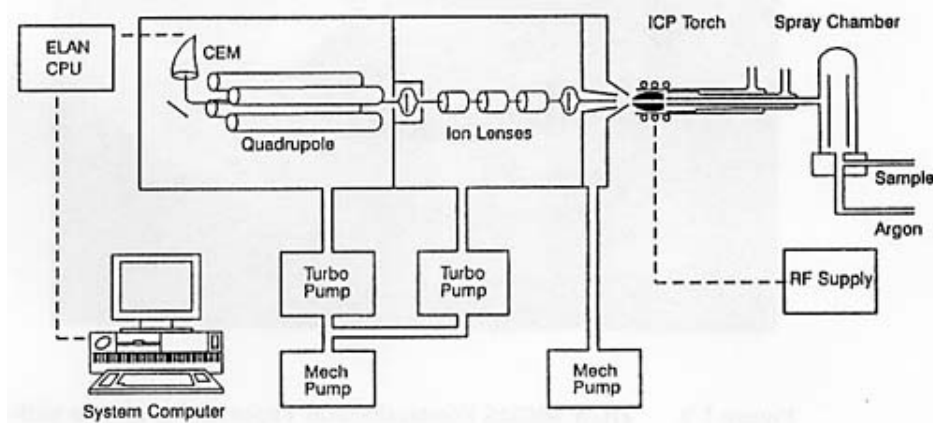


Figure 8 Schematic of ICP-MS detector  
([www.cco.caltech.edu](http://www.cco.caltech.edu))

The first article reporting elemental characterisation of NPs by ICP-MS focused on the elucidation of the Pb-to-Se ratio in PbSe nanocrystals (IwanMoreels, 2007 et al.). The ICP-MS results showed a biased 1:1 Pb-to-Se ratio consistent with a faceted spherical nanocrystal model of a quasi-stoichiometric PbSe core terminated by a Pb surface shell, with a systematic excess of Pb on the NP surface. Later, ICP-MS was used to determine the elemental content and distribution of Cd and Se in CdSe/ZnS quantum dots (QDs) during the synthesis of NPs. It is being used for the determination of NPs and their corresponding ionic forms in biological samples exposed with the aim to evaluate the different toxicity of both compounds.



ICP-MS cannot differentiate NPs or dissolved forms unless a physical separation is previously done. Only in a few cases, and very dependent on NP size and shape, the nebulization rate of ICP-MS can avoid the need to dissolve the nanoparticles. Some authors have used ICP-MS to determine quantum dots in mice, as a primary quantification method, by monitoring Cd isotopes. Single-walled carbon nanotubes (SWCNTs) can also be quantified by ICP-MS using CNT-associated nickel as the probe. Other NPs quantified by ICP-MS are gold and nickel NPs.

Several improvements have been proposed over the last few years for enhancing NP analysis using ICP-MS. One clear example is the introduction of single particle (sp)-ICP-MS for size distribution determination of NPs in colloidal suspensions. In single particle analysis, the analyte is spatially concentrated, in comparison to a solution of a soluble form of the same analyte. When one particle is introduced into the ICP, the atoms of the analyte produce a flash of gaseous ions in the plasma, which are measured as a single pulse by the detector. Meanwhile, the technique has been improved, e.g., by using micro-droplet sample introduction devices, to achieve better detection limits (Sabrina Gschwind, 2011 et al.). The principle of sp-ICP-MS is based on transient signal spike counting statistics of highly diluted samples, which requires a fast data acquisition.

The major advantage of sp-ICP-MS is the relatively low instrumental effort, which makes the technique easily accessible in every ICP-MS laboratory. However, sp-ICP-MS analysis is limited by the time resolution of the mass spectrometer used. Another recent analytical strategy is the detection by ICP-MS using isotopically modified NPs. This procedure allows low detection limits and an adequate monitoring of their fate and transformation in the sample of interest. In addition, recently new NPs, using a customized electrospray-differential mobility analyzer (ES-DMA) to achieve real-time upstream size discrimination before ICP-MS detection. DMA, also known as scanning ion mobility spectrometry, is a high-resolution size classification technique relevant to the analysis of discrete (dispersed) nano-scale species such as NPs, viruses, proteins and DNA.

### **Hyphenated Techniques:**

For characterization of ENM's especially metal-containing NPs one should adopt any one of these hyphenated techniques. They are FFF-ICP-MS, AF4-ICP-MS, AF4-sp-ICP-MS, HDC-ICP-MS or HDC-sp-ICP-MS. Studies were carried out on separation of AgNPs from aqueous matrices detected and quantified nano-Ag in untreated wastewater (influent) using

online AF4-ICP-MS method and the limit of detection (LOD) for the analysis was found to be 0.8 ng/L. The schematic of AF4-ICP-MS for analysis of AgNps with online addition of UV/vis detector is as shown below in figure (MdEhsanulHoque, 2012 et al. and Philippe A, 2014 et al.) monitored the agglomerations of polystyrene NPs using HDC and simultaneously gold colloid concentration and size are determined using ICP-MS. Analysis using HDC-ICP-MS for organic and inorganic colloids in synthetic surface water and ZnO, TiO<sub>2</sub>Nps in commercial sunscreens was carried out. Hence concluded that HDC-ICP-MS is a flexible, sensitive and reliable method to measure the size and the concentration of inorganic colloids in complex media and suggest that there may be a promising future for the application of HDC in environmental science.

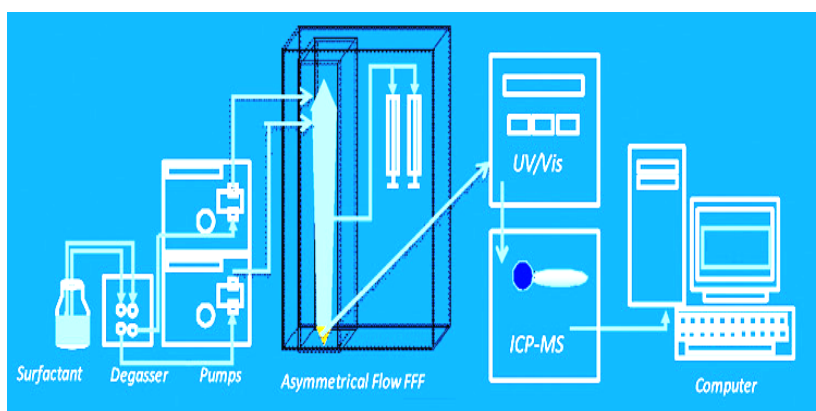


Figure 9 Schematic of AF4-ICP-MS with online UV/Vis detector (ICP-MS Technology, PerkinElmer, Inc.)

A simple approach for the simultaneous quantification of particle size, mass concentration, particle number concentration (PNC), and intended/extraneous elemental composition (all in a single analytical run) is described known as hydrodynamic chromatography-post-column injection-inductively coupled plasma mass spectrometry (HDC-PCi-ICP-MS).. The analytical system was based on the HDC-ICP-MS arrangement first applied to nano characterisation by Tiede et al., and further developed to include analysis in 'single particle' mode, by Pergantis and co-workers. An additional HPLC pump and injection port has been incorporated into the HDC-ICP-MS system, allowing aliquots of NIST-traceable ionic standards (and sample) to be added directly into the post-column flow, just prior to the detector. From this simple configuration, it will be shown that: particle mass concentration can be accurately quantified against a calibration curve constructed 'per sample' from the response obtained from the aliquots of standards, particle



size data can be obtained by direct comparison of sample retention times against that of reference standards; particle number concentration can be calculated from size data and mass data, on-column losses can be determined by comparison of on-column and post-column injected aliquots of sample (D.J.lewis, 2014). The system was validated using a silver nanoparticle test material which had been used in other published research (Loeschner K, 2013 et al.).

### **Conclusion:**

AF4 is the best separation technique of all the fractionation and chromatographic techniques for separating NPs on size basis. However channel miniaturization inhibits its accuracy. HDC for separation results worthy in lower concentrations of ENMs. AF4-ICP-MS is the reliable technique used to separate mixtures of NPs with significantly great resolution than HDC-ICP-MS. However large recovery ranges are observed for HDC-ICP-MS compared to AF4-ICP-MS. HDC-ICP-MS provides an additional benefit over AF4-ICP-MS by proving capable of separating dissolved signal from NP sample. Hence HDC-ICP-MS is advantageous over all hyphenated techniques to characterize nanomaterials analytically in environmental matrices. Hence this technique may be adopted to remove ENMs in wastewater treatment from activated sludge, and STP influents. However there is a need for research on practical implications to establish this technique for the wastewater treatment.

### **References:**

Nicole C. Mueller and Bernd Nowack (2008) Exposure modelling of engineered nanoparticles in the environment. *J Environ. Sci. Technol.* 42, 4447–4453.

Fadri Gottschalk, Elias Kost, and Bernd Nowack (2013) Engineered nanomaterials in water and soils: a risk quantification based on probabilistic exposure and effect modelling. *J Environmental Toxicology and Chemistry*, 32(6), 1278–1287.

Troy M. Benn and Paul Westerhoff (2008) Nanoparticle Silver Released into Water from Commercially Available Sock Fabrics. *Environ. Sci. Technol.* 42, 4133–4139.



Gottschalk F, Sonderer T, Scholz RW, Nowack B (2011) Modeled environmental concentrations of engineered nanomaterials (TiO<sub>2</sub>, ZnO, Ag, CNT, Fullerenes) for different regions. *Environ Sci. Technol.* 43, 9216–9222.

Christine Ogilvie Hendren, Appala R. Badireddy, Elizabeth Casman, Mark R. Wiesner (2013) Modeling nanomaterial fate in wastewater treatment: Monte Carlo simulation of silver nanoparticles (nano-Ag). *Science of the Total Environment.* 449, 418–425.

S. Gavankar, S. Suh, A.A. Keller (2014) Life cycle assessment of engineered nanomaterials. *Health and Environmental Safety of Nanomaterials*. Doi: 10.1533/9780857096678.2. 112.

Tian Yin Sun, Fadri Gottschalk, Konrad Hungerbühler, Bernd Nowack (2014) Comprehensive probabilistic modelling of environmental emissions of engineered nanomaterials. *Environmental Pollution.* 185, 69-76.

Ana Lopez-Serrano, Riansares Munoz Olivas, Jon SanzLandaluze and Carmen Camara (2014) Nanoparticles: a global vision. Characterization, separation, and quantification methods. *Potential environmental and health impact. Anal. Methods.* 6, 38-56.

Marcus. N Myers (1997) Overview of Field-Flow Fractionation. *CCC* 1040-7685/97/030151-58.

Korin D. Caldwell, Bruce J. Compton, J. Calvin Giddings and Randall J. Olson (1984) Sedimentation Field-flow Fractionation: A Method for Studying Particulates in Cataractous Lens. *Investigative Ophthalmology & Visual Science.* 25, 153-159.

Schimpf ME, Caldwell KD, Giddings JC, editors (2000) *Field-flow fractionation handbook*. New York: Wiley.

Jana Plockova, Josef Chmelik (1999) Different elution modes and field programming in gravitational field-flow fractionation: 2. Experimental verification of the range of conditions for flow-rate and carrier liquid density programming. *J. of Chromatography.* 868(2), 217-227.

Karl Gustav Wahlund, J. Calvin Giddings (1987) Properties of an asymmetrical flow field-flow fractionation channel having one permeable wall, *Anal. Chem.* 59(9), 1332–1339.



M. Baalousha, B. Stolpe, J.R. Lead (2011) Flow field-flow fractionation for the analysis and characterization of natural colloids and manufactured nanoparticles in environmental systems: A critical review. *J. of Chromatography A*. 1218(27), 4078–4103.

Sun Tae Kim, Dong Young Kang , Seungho Lee , Won-Suk Kim , Jong Taik Lee , Hye Sung Cho & Sang Ho Kim (2007) Separation and Quantitation of Silver Nanoparticles using Sedimentation Field-Flow Fractionation, *J. of Liquid Chromatography & Related Technologies*. 30(17), 2533-2544.

DosRamos JG, Silebi CA (1990) The determination of particle size distribution of submicrometer particles by capillary hydrodynamic fractionation (CHDF). *J Colloid Interface Sci*. 135, 165–177.

Striegel AM, Brewer AK (2012) Hydrodynamic Chromatography. *Annu Rev, Anal Chem*. 5, 15–34.

Penlidis A, Hamielec A, MacGregor J (1983) Hydrodynamic and Size Exclusion Chromatography of Particle Suspensions-An Update. *J Liq Chromatography*.6, 179–217.

IwanMoreels,Karel Lambert, José C. Martins, David De Muynck, Guy Allan, Frank Vanhaecke, and Zeger Hens, Dirk Poelman (2007), Composition and Size-Dependent Extinction Coefficient of Colloidal PbSe Quantum Dots, *Chem. Mater*. 19,6101–6106.

Sabrina Gschwind, Luca Flamigni, Joachim Koch, Olga Borovinskaya, Sebastian Groh, Kay Niemax and Detlef Günther (2011) Capabilities of inductively coupled plasma mass spectrometry for the detection of nanoparticles carried by monodispersemicrodroplets. *J. Anal. At.Spectrom.*, 26, 1166–1174.

MdEhsanulHoque , KambizKhosravi, Karla Newman, Chris D. Metcalfe (2012) Detection and characterization of silver nanoparticles in aqueous matrices using asymmetric-flow field flow fractionation with inductively coupled plasma mass spectrometry. *J. of chromatography*. 1233, 109-115.

Philippe A, Schaumann GE (2014) Evaluation of Hydrodynamic Chromatography Coupled with UV-Visible, Fluorescence and Inductively Coupled Plasma Mass Spectrometry Detectors for Sizing and Quantifying

---



---

Colloids in Environmental Media. PLoS ONE 9(2), e90559.  
DOI:10.1371/journal.pone.0090559

D. J. Lewis (2014) Hydrodynamic chromatography – inductively coupled plasma mass spectrometry, with post-column injection capability for simultaneous determination of nanoparticle size, mass concentration and particle number concentration (HDC-PCi-ICP-MS). Analyst, DOI: 10.1039/c4an01979b

Loeschner K , Navratilova J, Købler C, Mølhav K, Wagner S, von der Kammer F, Larsen EH (2013) Detection and characterization of silver nanoparticles in chicken meat by asymmetric flow field flow fractionation with detection by conventional or single particle ICPMS. Anal Bioanal Chem. 405(25)8185-8195.